RESEARCH ARTICLE

Nanog induces suppression of senescence via down-regulation of $p27^{KIP1}$ expression

Bernhard Münst[1,5,*], Marc Christian Thier[1,6,*], Dirk Winnemöller[1,7,*], Martina Helfen[1,7], Rajkumar P. Thummer[1,4‡], and Frank Edenhofer[1,2,3‡]

[1]Stem Cell Engineering Group, Institute of Reconstructive Neurobiology, University of Bonn - Life & Brain Center and Hertie Foundation, Sigmund-Freud Str. 25, 53127 Bonn, Germany
[2]Stem Cell and Regenerative Medicine Group, Institute of Anatomy and Cell Biology, Julius-Maximilians-University Würzburg, Koellikerstrasse 6, 97070 Würzburg, Germany
[3]Department of Genomics, Stem Cell Biology & Regenerative Medicine, Institute of Molecular Biology, Leopold-Franzens-University Innsbruck, Technikerstraße 25, 6020 Innsbruck, Austria.
[4]Department of Biosciences and Bioengineering, Indian Institute of Technology Guwahati, Guwahati 781039, Assam, India.
[5]Present address: Merck Life Science GmbH, Lilienthalstr. 16, 69214 Eppelheim, Germany.
[6]Present address: Division of Stem Cells and Cancer, Deutsches Krebsforschungszentrum (DKFZ), Im Neuenheimer Feld 280, 69120 Heidelberg, Germany.
[7]Present address: Miltenyi Biotec, Friedrich-Ebert-Str. 68, 51429 Bergisch Gladbach, Germany

[*]These authors contributed equally to this work.

‡Authors for correspondence (frank.edenhofer@wuerzburg.de; rthu@iitg.ernet.in; www.reprogramming.eu)

KEY WORDS: Embryonic stem cell, Protein transduction, Pluripotency, Senescence, Cell reprogramming, $p27^{KIP1}$

Journal of Cell Science • Advance article

ABSTRACT

A comprehensive analysis of the molecular network of cellular factors establishing and maintaining pluripotency as well as self renewal of pluripotent stem cells is key for further progress in understanding basic stem cell biology. Nanog is necessary for the natural induction of pluripotency in early mammalian development but dispensable for both, its maintenance as well as its artificial induction. To gain further insight into the molecular activity of Nanog we analyzed the gain-of-function of Nanog in various cell models employing a recently developed biologically active recombinant cell-permeant protein, Nanog-TAT. We found that Nanog enhances proliferation of both, NIH 3T3 as well as primary fibroblast cells. Nanog transduction into primary fibroblasts results in suppression of senescence-associated β-galactosidase activity. Investigation of cell cycle factors revealed that transient activation of Nanog correlates with consistent down-regulation of cell cycle inhibitor $p27^{KIP1}$. By chromatin immunoprecipitation analysis we confirmed bona fide Nanog binding sites upstream to the $p27^{KIP1}$ gene, establishing a direct link between physical occupancy and functional regulation. Our data demonstrates that Nanog enhances proliferation of fibroblasts via transcriptional regulation of cell cycle inhibitor p27 gene.

INTRODUCTION

Pluripotent stem cells, such as embryonic stem (ES) and induced pluripotent stem (iPS) cells, have tremendous potential in developmental biology as well as regenerative medicine due to their unlimited self renewal and unrestricted differentiation capacity. A thorough understanding of the molecular network of cellular factors, extracellular and intracellular signaling pathways, cell cycle regulation and microenvironment establishing and maintaining self-renewal, pluripotency is key for the development of biomedical applications of stem cells (Boyer et al., 2005; Cox et al., 2011; Loh et al., 2006; Lowry and Quan, 2010). Establishment and maintenance of stem cell identity particularly pluripotency is regulated by a core network of transcription factors. Oct4, Sox2 and Nanog belong to this transcriptional circuit that plays a pivotal role in self-renewal and maintenance of pluripotency (Chen et al., 2008; Chambers and Tomlinson, 2009; He et al., 2009; Pauklin et al., 2011). In concert with Oct4 and Sox2, Nanog governs pluripotent features in mouse and human cells (Boyer et al., 2005; Loh et al., 2006) by occupying the promoters of active genes encoding transcription factors, signal transduction components, and chromatin-modifying enzymes. Expression of Oct4 and Sox2 is relatively homogeneous in pluripotent cells whereas Nanog exhibits a heterogeneous expression (Singh et al., 2007), with cells having elevated levels of Nanog exhibiting efficient self-renewal.

The homeodomain transcription factor Nanog is expressed at early embryonic development, in the inner cell mass, in ES cells as well as the in developing germline in mammals (Chambers et al., 2003; Chambers et al., 2007; Mitsui et al., 2003). It has been shown that ES cells are sensitive to the dosage of Nanog. Overexpression of Nanog is sufficient to prevent the differentiation in ES cells in absence of feeders and vital extracellular growth factors (Chambers et al., 2003; Darr et al., 2006; Mitsui et al., 2003). Downregulation of Nanog in ES cells results in loss of pluripotency, reduction in cell proliferation and differentiation towards extraembryonic lineages (Chambers et al., 2003; Hyslop et al., 2005; Ivanova et al., 2006; Mitsui et al 2003; Zaehres et al., 2005). Additionally, cell fusion experiments demonstrate that Nanog promotes the formation of pluripotent hybrids as Nanog stimulates pluripotent gene activation in neural stem cells, thymocytes and fibroblasts in a dose-dependent manner (Silva et al., 2006). Knockout studies revealed that Nanog is dispensable for the housekeeping machinery of pluripotency since the conditional deletion of Nanog in ES cells does unexpectedly not result in loss of pluripotency (Chambers et al., 2007). During development *in vivo*, pluripotency is not established without Nanog and inner cell mass cells are trapped in an intermediate stage (Silva et al., 2009) assigning Nanog an

essential role for the natural acquisition but not the maintenance of pluripotency (Pan and Thomson, 2007; Saunders et al., 2013). Thus, a well-defined role of Nanog in self-renewal and natural induction of pluripotency at molecular level remains to be investigated.

Inducible gain-of-function systems permitting a precise control over time and dosage of gene products allow straightforward studies of stemness and cell reprogramming pathways at the molecular level. Using protein transduction, we generated cell-permeant versions of core pluripotency factors Oct4 and Sox2 proteins (Bosnali & Edenhofer, 2008) to generate iPS cells (Thier et al., 2010; Thier et al., 2012a) and induced neural stem (iNS) cells (Thier et al., 2012b). Recently, we reported a cell-permeant version of Nanog and demonstrated that it promotes ES cell proliferation and self-renewal in absence of leukemia inhibitory factor by inhibiting endodermal specification in a Stat3-independent manner (Peitz et al., 2014). Here we set out to study the function of Nanog in somatic cells as a means to analyze its contribution for self-renewal in cells in general and ES cells in particular. We show that biologically active cell-permeant Nanog induces enhanced proliferation in fibroblasts. Moreover, transient activation of Nanog consistently correlates with downregulation of cell cycle kinase inhibitor $p27^{KIP1}$. In addition, chromatin immunoprecipitation (ChIP) analysis reveals two distinct putative Nanog binding sites upstream to the $p27^{KIP1}$ gene. In conclusion, our data suggests that Nanog as a potential regulator of p27 gene to enhance proliferation of fibroblasts.

RESULTS

Nanog enhances proliferation of fibroblasts and induces anchorage-independent growth

We recently reported that cell-permeant recombinant Nanog protein enhances proliferation and maintains pluripotency of mouse ES cells by inhibiting endodermal specification in the absence of leukemia inhibitory factor (Peitz et al., 2014). Here we set out to use cell-permeant recombinant Nanog as a gain-of-function paradigm in various cellular models in order to assess a putative function of Nanog in somatic cells. NIH 3T3 cells are derived from the mouse embryo and exhibit a strictly contact-inhibited growth of spindle-shaped cells in culture. Nanog protein transduction into NIH 3T3 cells results in three-dimensional growth and formation of cell foci (Fig. 1A) indicating anchorage-independent growth. Foci formation is strictly dependent on the concentration and duration of exposure of Nanog-TAT (Fig. 1B,C). Maximal numbers of foci were observed upon application of 50nM Nanog-TAT for 5 days (Fig. 1C). In order to assess whether Nanog gain-of-function alone has an impact on the stem cell transcriptional network in NIH 3T3 cells we analyzed a set of pluripotency-

associated genes by RT-PCR. This analysis revealed that Nanog protein transduction had no impact on transcript levels of Oct4, Sox2 and Rex-1 (data not shown). To analyze the growth kinetics of Nanog-transduced NIH 3T3 cells we determined cumulative cell numbers for 10 days. Nanog-TAT caused a strongly increased proliferation yielding about 4-fold more cells within 10 days as compared to the control (Fig. 1D). To rule out putative pleiotropic effects associated with the direct delivery of recombinant protein, we employed a cell-permeant Nanog control protein lacking the homeodomain, designated ΔNanog-TAT. ΔNanog-TAT failed to enhance proliferation of NIH 3T3 cells as determined by cumulative cell numbers after 10 days of treatment as well as by quantification of foci formation (Fig. S1). To confirm the anchorage-independent growth phenotype induced by full-length Nanog we assayed the capability of Nanog-TAT-treated cells to grow in soft agar. The number and sizes of the resulting colonies were quantified after 19 days. Nanog protein transduction resulted in growth of more than 250 colonies in a 6 cm dish, 20% of them exceeding a diameter of 200 µm, whereas only few colonies were observed in case of the control (Fig. 1E,F). Both, foci formation and growth in soft agar, indicate contact independent growth due to Nanog activity.

Oncogenes like *ras* are able to stably and irreversibly transform NIH 3T3 cells and we asked whether the transient intracellular delivery of Nanog results in stable transformation as well or represents a transiently occurring phenotype. To address this question, we applied Nanog-TAT for a period of 8 days to NIH 3T3 cells, which led to foci formation. Cells were then passaged and cultured in the presence or absence of Nanog-TAT. The foci formed in the presence of Nanog-TAT were no longer detected after withdrawal of Nanog-TAT, indicating that the transforming effect is a reversible process (Fig. 1G). It has been reported that the overexpression of *Eras* induces a similar oncogenic transformation in somatic cells (Takahashi et al., 2003) involving the Phosphatidylinositol 3-kinase (PI3K) cascade, which is known to be important for both, transformation (Rodriguez-Viciana et al., 1997) and ES cell propagation (Di Cristofano et al., 1998; Sun et al., 1999). Thus, we examined whether PI3K inhibition does interfere with Nanog protein transduction. It turned out that Nanog-TAT is not able to rescue the growth-inhibiting effect of PI3K suggesting that Nanog depends on PI3K activity (Fig. 1H). In contrast, the transforming property of Nanog-TAT was only slightly affected by PI3K inhibition. The ability to form foci was largely maintained although foci formation was retarded due to the reduced proliferation of the cells (Fig. 1I). In conclusion, our results demonstrate that Nanog induces loss of contact inhibition by a PI3K-independent mechanism in NIH3T3 cells.

Next we studied the activity of Nanog protein in murine embryonic fibroblasts (Oct4-GiP MEF) representing primary, non-transformed cell population. Nanog transduction induced enhanced proliferation and morphological changes of low passage Oct4-GiP MEFs to a more bipolar shape with an increased nuclear-cytoplasmic ratio (Fig. 1J). During long-term culture control Oct4-GiP MEFs transitionally ceased to proliferate after 4-6 passages, but then resumed expansion indicative of spontaneous transformation of the cells. Nanog-TAT-treated Oct4-GiP MEFs in contrast kept dividing for at least 13 passages (more than 3.5 months) (Fig. 1K. To check the chromosomal integrity we examined the karyotypes of untreated Oct4-GiP MEF cultures (passage 3) and long-term-cultured cells (passage 14) incubated with or without Nanog-TAT (Fig. 1L). We observed that all metaphases of untreated high-passage cells adopted an aberrant mainly hypo-tetraploid karyotype. Nanog-transduced cells, in contrast, predominantly maintained a normal karyotype, indicating that prolonged expansion of Nanog-TAT treated cells is not a cause of aneuploidy.

Nanog suppresses replicative senescence in human primary fibroblasts

Next we investigated to which extent Nanog has the same effect on primary human cells. With human primary adult dermal fibroblasts (MP-hADF) we observed an increased proliferation rate after Nanog transduction, which mirrors the effect observed in MEFs. Nanog-TAT-treated cells grew densely packed and adopted more spindle-like shape and the ratio of cytoplasm to nucleus declined. From a starting cell number of 250,000 cells, Nanog-TAT treated fibroblasts exhibit a final cumulative cell number of $8x10^{11}$ after 10 passages. In contrast, 250,000 MP-hADF fibroblast cells cultured with control medium only give rise to $1.5x10^{9}$ after 10 passages (Fig. 2A). We reasoned that the capability to enhance proliferation over extended passages might be due to Nanog-induced suppression of replicative senescence. In order to analyze senescence in Nanog-transduced cells we determined senescence-associated β-galactosidase (SA-β-gal) activity as a means to quantify senescent cells in culture (Dimri et al., 1995). About 6% of MP-hADF cultured under normal conditions for 3 passages stained positive for SA-β-gal (Fig. 2B,C). In contrast, no SA-β-gal activity was detectable in MP-hADF cultured in the presence of Nanog-TAT (Fig. 2B,C). These data demonstrate that Nanog activity is able to suppress senescence in primary fibroblast cells.

Culture of MEFs with Nanog-TAT decreases p27^{KIP1} expression

In order to investigate the senescence-blocking effect induced by Nanog at molecular level we analyzed the expression of cell cycle factors. For this, Oct4-GiP MEFs were cultured in low serum conditions for G0 phase synchronization and treated thereafter with aphidicolin in order to synchronize the cell population in S phase of the cell cycle. Oct4-GiP MEFs were cultured with control medium and Nanog-TAT, respectively. After 5, 8, and 21 hours cells were harvested and subjected to RT-PCR analysis. We analyzed a set of cell cycle factors including p53, p16^{INK4a}, p21$^{CIP/WAF}$ and p27^{KIP1}. p53 is involved in DNA repair as well as initiation of apoptosis in case DNA damage is irreparable. p16^{INK4a} is one marker that can be used for the identification of a senescent phenotype in cells. p21$^{CIP/WAF}$ and p27^{KIP1} are proteins of the Cip/Kip family that are key cell cycle regulators by inhibiting Cdk2. Besides this, p21$^{CIP/WAF}$ acts downstream of p53 in regulating transition through the cell cycle in G1 phase (El-Deiry et al., 1994). FGF receptor expression can indicate for a proliferative status in fibroblast cells. RT-PCR analysis demonstrated that Nanog protein transduction did not yield a significant modulation of the analyzed cell cycle factors except a modest down-regulation of p27^{KIP1} (Fig. S2A). After 5 hours of Nanog-TAT treatment the RNA expression level of p27^{KIP1} is slightly reduced to about 90% compared to fibroblasts cultured in control medium. 8 hours of Nanog-TAT application diminishes the expression of p27^{KIP1} to around 70%. After 21 hours of Nanog transduction we detected only about 25% p27^{KIP1} transcript as compared to cells incubated with control media (Fig. S2A). To further determine the p27^{KIP1} modulation quantitatively RT-qPCR analysis was performed. MEFs were synchronized in S phase of the cell cycle and cultured with control medium and 100 nM Nanog-TAT for 2.5, 5 and 10 hours. Cells were then harvested and subjected to RT-qPCR analysis. We observed gradual down-regulation of p27^{KIP1} mRNA upon Nanog-TAT treatment (Fig. S2B). In order to further assess cell cycle factor modulation also at protein level, cell lysates were prepared after 5 and 24 hours of Nanog transduction and subjected to immunoblot analysis. Immunoblotting analysis confirmed that out of the factors analyzed p27^{KIP1} is consistently expressed at lower levels after both, 5 and 24 hours of Nanog transduction (Fig. 2D,E). Quantification demonstrates that 5 hours of Nanog transduction is sufficient to reduce the p27^{KIP1} protein level to about the half. 24 hours of incubation with Nanog-TAT yielded a further decline of p27^{KIP1} to about 40% (Fig. 2E). In contrast Nanog transduction has no apparent effect on p21$^{CIP/WAF}$, p53 and Cyclin D1 levels. To further assess the specificity of this effect we employed the ΔNanog-TAT protein as a control. It turned out that ΔNanog-TAT did not result in downregulation of

p27^{KIP1} expression at any time point investigated (Fig. 2F).

ChIP analysis reveals Nanog binding sites within the p27^{KIP1} locus

Thus far, our data indicate that Nanog is able to enhance proliferation and to suppress senescence in somatic cells, along with consistently reduced p27^{KIP1} levels. We further asked whether p27^{KIP1} is a direct transcriptional target of Nanog explaining the observed downregulation of p27^{KIP1}. Two studies using high-resolution massive parallel DNA sequencing of chromatin immunoprecipitation (ChIP-seq) reported two Nanog binding sites in the upstream region of the p27^{KIP1} gene (Fig. 3A; Chen et al., 2008; Marson et al., 2008). To confirm Nanog binding to these sites, designated 'D (primer pairs designated as D1 and D2)' and 'P (primer pairs designated as P1 and P2)' in the following, we performed ChIP analysis using mouse ES cells. Oct4-GiP MEF cells served as a negative control since they do not express Nanog. ChIP analysis with a Nanog specific antibody revealed amplification of Nanog bound regions D and P upstream to the p27^{KIP1} as judged by both, semi-quantitative PCR (Fig. 3B) and q-PCR analysis (Fig. 3C). Amplification was not observed using the Oct4-GiP MEF control cells, beads only as well as unspecific IgG. Moreover, specificity is confirmed by the observation that a desert control lying within the p27^{KIP1} gene was not amplified (Fig. 3B). This observation confirms Nanog binding sites in the upstream region of the p27^{KIP1} gene.

To demonstrate the binding of Nanog to these p27^{KIP1} upstream regions in fibroblasts after protein transduction as well we applied 100nM of Nanog-TAT to Oct4-GiP MEFs. Oct4-GiP MEF cells treated with vehicle only served as a negative control. ChIP analysis employing a Nanog-specific antibody showed amplification of Nanog-bound regions upstream to the p27^{KIP1} gene only in Oct4-GiP MEF cells transduced with Nanog (Fig. 3D). This data demonstrates that Nanog binds to the upstream region of the p27^{KIP1} gene in Nanog-TAT transduced fibroblasts indicating direct regulation of its expression.

DISCUSSION

In this study we set out to analyze a putative function of the pluripotency factor Nanog in somatic cells. We employed a cell-permeant version of Nanog as a non-DNA based, non-genetic paradigm to modulate cellular function. We found that Nanog protein transduction enhances proliferation of both, NIH 3T3 as well as primary mouse and human fibroblasts. Moreover, Nanog induces anchorage-independent growth of NIH 3T3 cells in a dose- and time-dependent manner, otherwise typically exhibiting strict contact inhibition.

Previously it has been reported that genetic ectopic expression of Nanog in NIH 3T3 cells shows an enhanced proliferation (Zhang et al., 2005) and foci formation as well as growth in soft agar (Piestun et al., 2006). Nanog has also been reported to enhance proliferation and/or self-renewal in other somatic and stem cell lines by regulating molecules involved in stemness, cell cycle and senescence machinery (Cao et al., 2010 (adult human fibroblasts); Choi et al., 2012 (embryonic carcinoma cells); Go et al., 2008 (mesenchymal stem cells); Shan et al., 2012 (cancer stem cells); Tanaka et al., 2007 (hematopoietic stem cells)). Thus, we conclude that our Nanog gain-of-function paradigm by direct protein delivery is functional and induces loss of contact inhibition and gain in proliferation. Moreover, we demonstrate that PI3K inhibition does not substantially affect induction of anchorage-independent growth, whereas Nanog is not able to overcome the growth-inhibiting effect induced by PI3K inhibition. In primary fibroblasts, Nanog protein transduction induces enhanced proliferation enabling prolonged culture for more than 13 passages seemingly bypassing cellular senescence. Indeed, we show that Nanog transduction into primary human fibroblasts results in effective suppression of SA-β-gal activity, a widely used marker for senescence. The expansion of primary human cells by transient transduction of Nanog protein might be of general interest, in particular for in vitro expansion of cells.

Our study shows that Nanog protein transduction in mouse fibroblasts specifically results in low expression of $p27^{KIP1}$ both, at RNA and protein level, indicating a functional link between the pluripotency transcriptional network and the cell cycle machinery. We confirmed two putative Nanog binding sites in the 5'-UAS of the $p27^{KIP1}$ gene (Chen et al., 2008; Marson et al., 2008) by ChIP analyses both, in ES cells and Nanog-transduced MEF cells. Recently, it has been reported that Oct4 represses p21 expression to contribute to ES cell proliferation and self-renewal (Lee et al., 2010). $p27^{KIP1}$ together with $p21^{CIP/WAF}$ represent the major cyclin-dependent kinase inhibitors (CKIs) regulating G1 to S transition. Ablation of $p27^{KIP1}$ in mice results in multiorgan hyperplasia (Fero et al. 1996) and numerous studies *in vitro* confirm a regulatory control of $p27^{KIP1}$ over proliferation. Notably, ES cells do lack the ability to undergo senescence and their growth is not subject to contact inhibition or anchorage dependence. Given our observation that Nanog gain-of-function is able to suppress contact inhibition and senescence while down-regulating $p27^{KIP1}$ we provide a functional link between Nanog and cell cycle regulator p27 gene at molecular level.

MATERIALS AND METHODS

Cell culture

NIH 3T3 MEF, Oct4-GiP MEF and primary human adult dermal MP fibroblasts (MP-hADF) were cultured in Dulbecco's modified Eagle medium (DMEM, GIBCO, Life Technologies, Paisley, UK) containing 10% fetal calf serum (FCS; GIBCO, Life Technologies, Paisley, UK) and 100 U/ml penicillin and 0.1 mg/ml streptomycin (GIBCO, Life Technologies, Paisley, UK). In all experiments medium was changed daily. Culture of Oct4-GiP ES cells (Oct4-GiP; Ying et al., 2002) for ChIP analysis was performed on 0.1% gelatin-coated (Sigma-Aldrich, St Louis, MO) dishes in high glucose DMEM (GIBCO, Life Technologies, Paisley, UK) with 15% FCS, 1% non-essential amino acids (GIBCO, Life Technologies, Paisley, UK), 1 mM sodium pyruvate (GIBCO, Life Technologies, Paisley, UK), 2 mM L-glutamine (GIBCO, Life Technologies, Paisley, UK) and 100 µM β-mercaptoethanol (GIBCO, Life Technologies, Paisley, UK) and 1000 U/ml Leukemia Inhibitory Factor (LIF; Millipore, Temecula, CA, USA). Differentiated cells were counter-selected from Oct4-GiP ES cells by adding 1 µg/ml puromycin (GIBCO, Life Technologies, Karlsruhe, Germany) for at least one week before an experiment.

For growth curve analysis of Oct4-GiP MEF cells, 20,000 cells exhibiting passage number 1 were plated in a 3.5 cm^2 dish and cultured in the absence and presence of 50-100 nM Nanog-TAT over several passages. As soon as cells reached 80-90% confluency, the cells were sub-cultures and again 20,000 cells were replated. After each passage, cells were counted and the cumulative cell numbers were determined in order to assess the proliferation rate.

For growth curve analysis of MP-hADF cells, 250,000 cells were seeded in a 6 cm dish and cultured in the absence and presence of 100 nM Nanog-TAT over several passages. As soon as cells reached 80-90% confluency, the cells were splitted and again 250,000 cells were re-seeded. After each passage, cells were counted and the cumulative cell numbers were determined in order to assess the proliferation rate.

For cell proliferation analysis of Oct4-GiP MEFs cultured with Nanog-TAT, ΔNanog-TAT or control medium via RT-PCR or immunoblot, 750,000 cells exhibiting passage number 5 were seeded on a 10 cm cell culture dish. In order to synchronize the fibroblasts, cells underwent serum starvation, i.e. a concentration of 0.2% FCS, for 48 hours. This led to an accumulation of cells in G0 phase of the cell cycle. Subsequently Oct4-GiP MEFs were cultured in MEF medium containing 10% FCS, but the medium was

supplemented with 4 µg/mL aphidicolin (Sigma-Aldrich, St. Louis, MO, USA) for another 16 hours to finally synchronize cells in S phase of the cell cycle. Afterwards Oct4-GiP MEFs were washed twice with PBS and cultured with 100 nM of Nanog-TAT, 50 nM of ΔNanog-TAT or control medium for the indicated time points.

Plasmid construction and preparation of recombinant fusion proteins

Plasmid generation of the pTriEx1.1 vector harboring the genetic information of Nanog-TAT (NLS-Nanog-TAT-H6) for expression and native purification of recombinant protein is described elsewhere (Peitz et al., 2014). For NLS-ΔNanog-TAT-H6 (without the 60 aa long homeodomain), PCR fragments encompassing the open reading frames for NLS-ΔNanog-TAT-H6 (hereafter ΔNanog-TAT) flanked by NcoI-XhoI sites were synthesized and inserted into the NcoI-XhoI sites of pTriEx1.1 (Novagen, UK). Native purification of ΔNanog-TAT was performed as described elsewhere for Nanog-TAT (Peitz et al., 2014) with some modifications. For bacterial over-expression of ΔNanog-TAT, overnight cultures (LB containing 0.5% glucose and 50 µg/mL Carbenicillin) were inoculated with freshly transformed BL21 (DE3) GOLD cells (Stratagene, La Jolla, CA, USA) and cultured at 30°C. Expression cultures (TB containing 0.5% glucose and 100 µg/ml Ampicillin) were grown at 37°C and induced at an OD_{600} of 1.5 with 0.5 mM Isopropyl-β-D-thiogalactopyranoside (IPTG) for 1h. Pellets were resuspended in lysis buffer (2 mM imidazole, 500 mM NaCl, 50 mM Na_2HPO_4, 5 mM Tris, pH 7.8) and lysozyme (Sigma-Aldrich, St. Louis, MO, USA) and benzonase (Novagen, UK) was sequentially added, each for 20 minutes at 4°C. After a centrifugation step the supernatant was incubated for 1h with 1 ml Ni-NTA slurry (Qiagen, Hilden, Germany) per liter initial culture. The resin was packed in a gravity column, washed (100 mM imidazole, 500 mM NaCl, 50 mM Na_2HPO_4, 5 mM Tris, pH 7.8) with 6 bed volumes and eluted (250 mM imidazole, 500 mM NaCl, 50 mM Na_2HPO_4, 5 mM Tris, pH 7.8) with 8 bed volumes. Eluted fractions were successively dialyzed against PBS followed by non-supplemented KnockOut-DMEM (GIBCO, Life Technologies, Paisley, UK).

Nanog protein transduction

Medium for transduction experiments was prepared by mixing Nanog dialysate fractions in a ratio of 1:1 with double supplemented medium (AdvDMEM (GIBCO, Life Technologies, Paisley, UK)) additionally supplemented with 2% FCS, 1% ITS (GIBCO, Life Technologies, Paisley, UK), 1% non-essential amino acids, 4 mM glutamine and 200 µM β-mercaptoethanol). The mixture was incubated in a water bath for 2h at 37°C and cleared from

precipitations by centrifugation and sterile filtration. FCS was then added to a final concentration of 5%. Final Nanog-TAT concentration in FCS containing medium was determined via dot blot analysis with Nanog-TAT dialysis fraction serving as standard.

Foci formation and soft agar assay

NIH 3T3 cells were grown in the presence of Nanog-TAT in 12 well plates and seeded at low density (10^3 cells/well). Untreated cells served as a control. Medium was changed every day. After 8 to 10 days 3-dimensional foci were counted. For soft agar assays 6 cm petri-dishes were covered with 5 ml of the appropriate medium containing 0.5% agarose. NIH 3T3 cells were pre-incubated with or without Nanog-TAT for 6 days. $1x10^4$ cells were suspended in 2 ml of the appropriate medium containing 0.3% agarose with or without Nanog-TAT (25-100 nM) and added to each plate. We added 1 ml of control medium or medium containing Nanog-TAT weekly, respectively. After 19 days of growth in soft agar the diameters of colonies were measured and numbers of colonies were counted.

SA β-Galactosidase (SA-β-gal) staining

For the analysis of SA-β-gal expression, MP-hADF at passage 16, already cultured with 100 nM of Nanog-TAT for 2 weeks were seeded at a density of 250,000 cells per 6 cm dish. The next day, cells were fixed and stained for SA-β-gal expression (Dimri et al., 1995).

Karyotype analysis

80% confluent Oct4-GiP MEFs were incubated with 0.1 µg/ml colcemid (Gibco® KaryoMAX® Colcemid™ Solution in HBSS; Grand Island, NY, USA) for 16 hours. Cells were then trypsinized and resuspended in hypotonic KCl solution (0.075M), incubated for 10 min at room temperature and fixed with methanol/glacial acetic acid (3:1). Chromosomes were visualized using Giemsa dye.

Western Blotting

For SDS-PAGE analysis, gels exhibiting a percentage of 10% or 15% (bis)acrylamide were used. SDS-PAGE separated protein samples were blotted onto a nitrocellulose membrane employing wet blot technique. Blotting was performed for 1h at 100V. For cell cycle analysis, we employed the following antibodies: $p21^{CIP/WAF}$ (556431; mouse IgG, 1:200, BD Pharmingen, Heidelberg, Germany), $p27^{KIP1}$ (554069; mouse IgG, 1:200, BD Pharmingen, Heidelberg, Germany), p53 (1C12; mouse IgG, 1:2000, Cell Signaling, Frankfurt, Germany),

and Cyclin D1 (DCS-6; mouse IgG, 1:200, BD Pharmingen, Heidelberg, Germany). Cyclin D1 exhibits an additional band in immunoblot analysis. This phenomenon observed is due to the rodent origin of cells, as stated in the datasheet provided by the manufacturer of the antibody. As secondary antibody, we utilized HRP-linked anti-mouse IgG (7076; 1:200–1:1000; Cell Signaling Technology, Frankfurt, Germany) antibody. Detection was carried out with SuperSignal West Pico Chemiluminescent Substrate (PIERCE; IL, USA) or Supersignal West Femto Chemiluminescent Substrate (PIERCE; IL, USA) respectively.

RT-PCR

RNA from aggregates or somatic cells was isolated with the SV Total RNA Isolation System (Promega, Madison, USA), RNeasy Mini Kit (Qiagen Inc., Hilden, Germany) or Trizol (Invitrogen), respectively, and reverse-transcribed with M-MLV Reverse Transcriptase, RNase H Minus, Point Mutant (Promega, Madison, USA) or iScript reverse transcriptase (Bio-Rad, Hercules, CA, USA). PCR reactions were performed using GoTaq (Promega, Madison, USA). Primers used for RT-PCR are listed in Supplementary Table S1.

Chromatin immunoprecipitation (ChIP)

For ChIP analysis, Oct4-GiP MEF, Oct4-GiP ES cells were used. Proteins bound to DNA were cross-linked using 1% formaldehyde for 7 min at room temperature followed by quenching the fixation reaction by addition of glycine (0.125 M final concentration) for 5 min at room temperature. After washing with ice-cold PBS, cells were collected by centrifugation and were lysed in lysis buffer (50 mM Tris-HCl (pH 8.1), 10 mM EDTA, 0.1% SDS and Complete protease inhibitors (Roche; IN, USA)) for 10 min on ice and further sonicated using Bioruptor (Diagenode; CA, USA), centrifuged and the supernatant was frozen at -80°C. The supernatant was thawed and 50 µg of chromatin was diluted 10 times in dilution buffer (16.7 mM Tris-HCl pH 8.0, 167 mM NaCl, 0.01% SDS, 1.1% Triton X-100, 1.2 mM EDTA and complete protease inhibitors). 5 µg (10%) of input was taken as a control. Followed by dilution, the protein-DNA complexes were immunoprecipitated overnight at 4°C with rotation using primary antibodies Nanog (AB5731, Millipore, USA) and rabbit control IgG ChIP grade (ab46540, Abcam, USA). Beads only were also taken as a negative control. Immunoprecipitated chromatin was incubated with Protein A/G Plus agarose beads (sc-2003; Santa Cruz Biotechnology, Santa Cruz, CA, USA) for another 1h at 4ºC and then washed 3 times with low salt washing buffer (20 mM Tris-HCl pH 8.0, 1% Triton X-100, 0.1% SDS, 150 mM NaCl, 2 mM EDTA, 0.01% Tween 20) and twice with high salt washing buffer (20

mM Tris-HCl pH 8.0, 1% Triton X-100, 0.1% SDS, 500 mM NaCl, 2 mM EDTA, 0.01% Tween 20). The protein-DNA complexes bound to the beads were eluted by incubation with elution buffer (1% SDS, 0.1M $NaHCO_3$) and subsequently treated with RNAse (2 hours; Concert^{TM}, Carlsbad, CA, USA) and Proteinase K (2 hours; Roche Mannheim, Germany). Cross-linking was then reversed by incubation overnight at 65°C. Bound DNA was purified by Wizard SV Gel and PCR clean-up kit (Promega, Madison, USA) and the eluted DNA was then used for both semi-quantitative and q-PCR for analysis. Quantitative real-time PCR (q-PCR) was performed using the SYBR-green Supermix (Bio-Rad, Hercules, CA, USA) on an Eppendorf realplex Mastercycler and the data was analyzed using fold enrichment method. Primers used for both semi-quantitative PCR and q-PCR to identify the putative Nanog protein binding sites to the $p27^{KIP1}$ genomic region regulating the $p27^{KIP1}$ expression and the desert control are listed in supplementary Table S2. Two biological replicates were performed for this experiment. ChIP analysis following the above protocol was also performed on Nanog-TAT transduced and non-transduced Oct4-GiP MEF (passage 3). Cells were washed with heparin (0.5 mg/ml in PBS; Sigma-Aldrich, St. Louis, MO, USA) to remove non-internalized protein before harvesting cells.

Statistical analysis

Statistical analysis to calculate p-value was carried out using a two-tailed test. The level of significance was set to $p < 0.05$.

Acknowledgements

We thank Shinya Yamanaka, Austin Smith and Ian Chambers for providing materials and scientific comments. We are grateful to Gunnar Schotta, University of Munich for helping with ChIP analysis. We thank Nicole Russ and Martina Gebhardt for excellent technical support.

Competing interests

The authors declare no potential conflicts of interest.

Author contributions

B.M., M.T., R.P.T. conception and design, collection and/or assembly of data, data analysis and interpretation, manuscript writing, and final approval of manuscript; D.W., M.H. conception and design, collection and/or assembly of data, data analysis and interpretation; F.E. conception and design, financial support, collection and/or assembly of data, data analysis and interpretation, manuscript writing, and final approval of manuscript.

Funding

This work was supported by grants from the Deutsche Forschungsgemeinschaft, DFG, (F.E.); the German Ministry of Education and Research, BMBF (F.E.); the European Union (F.E.) and by the IIT Guwahati Start-Up Grant (R.P.T.).

References

Bosnali, M. and Edenhofer, F. (2008). Generation of transducible versions of transcription factors Oct4 and Sox2. *Biol. Chem.* **389**, 851-61.

Boyer, L. A., Lee, T. I., Cole, M. F., Johnstone, S. E., Levine, S. S., Zucker, J. P., Guenther, M. G., Kumar, R. M., Murray, H. L., Jenner, R. G. et al. (2005). Core transcriptional regulatory circuitry in human embryonic stem cells. *Cell* **122**, 947-56.

Cao, J., Xiao, Z., Chen, B., Gao, Y., Shi, C., Wang, J. and Dai, J. (2010). Differential effects of recombinant fusion proteins TAT-OCT4 and TAT-NANOG on adult human fibroblasts. *Frontiers in Biology* **5**, 424-430.

Chambers, I. and Tomlinson, S. R. (2009). The transcriptional foundation of pluripotency. *Development* **136**, 2311-22.

Chambers, I., Colby, D., Robertson, M., Nichols, J., Lee, S., Tweedie, S. and Smith, A. (2003). Functional expression cloning of Nanog, a pluripotency sustaining factor in embryonic stem cells. *Cell* **113**, 643-55.

Chambers, I., Silva, J., Colby, D., Nichols, J., Nijmeijer, B., Robertson, M., Vrana, J., Jones, K., Grotewold, L. and Smith, A. (2007). Nanog safeguards pluripotency and mediates germline development. *Nature* **450**, 1230-4.

Chen, X., Xu, H., Yuan, P., Fang, F., Huss, M., Vega, V. B., Wong, E., Orlov, Y. L., Zhang, W., Jiang, J. et al. (2008). Integration of external signaling pathways with the core transcriptional network in embryonic stem cells. *Cell* **133**, 1106-17.

Choi, S. C., Choi, J. H., Park, C. Y., Ahn, C. M., Hong, S. J. and Lim, D. S. (2012). Nanog regulates molecules involved in stemness and cell cycle-signaling pathway for maintenance of pluripotency of P19 embryonal carcinoma stem cells. *J. Cell Physiol.* **227**, 3678-92.

Cox, J.L., Mallana, S.K., Ormsbee, B.D., Desler, M., Wiebe, M.S. and Rizzino, A. (2011). Banf1 is required to maintain the self-renewal of both mouse and human embryonic stem cells. *J. Cell Sci.* **124**, 2654-65.

Darr, H., Mayshar, Y. and Benvenisty, N. (2006). Overexpression of NANOG in human ES cells enables feeder-free growth while inducing primitive ectoderm features. *Development* **133**, 1193-201.

Di Cristofano, A., Pesce, B., Cordon-Cardo, C. and Pandolfi, P. P. (1998). Pten is essential for embryonic development and tumour suppression. *Nat. Genet.***19**, 348-55.

Dimri, G. P., Lee, X., Basile, G., Acosta, M., Scott, G., Roskelley, C., Medrano, E. E., Linskens, M., Rubelj, I., Pereira-Smith, O. et al. (1995). A biomarker that identifies senescent human cells in culture and in aging skin in vivo. *Proc. Natl. Acad. Sci. USA* **92**, 9363-7.

el-Deiry, W. S., Harper, J. W., O'Connor, P. M., Velculescu, V. E., Canman, C. E., Jackman, J., Pietenpol, J. A., Burrell, M., Hill, D. E., Wang, Y. et al. (1994). WAF1/CIP1 is induced in p53-mediated G1 arrest and apoptosis. *Cancer Res.* **54**, 1169-74.

Fero, M. L., Rivkin, M., Tasch, M., Porter, P., Carow, C. E., Firpo, E., Polyak, K., Tsai, L. H., Broudy, V., Perlmutter, R. M. et al. (1996). A syndrome of multiorgan hyperplasia with features of gigantism, tumorigenesis, and female sterility in p27(Kip1)-deficient mice. *Cell* **85**, 733-44.

Go, M. J., Takenaka, C. and Ohgushi, H. (2008). Forced expression of Sox2 or Nanog in human bone marrow derived mesenchymal stem cells maintains their expansion and differentiation capabilities. *Exp. Cell Res.* **314**, 1147-54.

He, S., Nakada, D. and Morrison, S. J. (2009). Mechanisms of stem cell self-renewal. *Annu Rev Cell Dev. Biol.* **25**, 377-406.

Hyslop, L., Stojkovic, M., Armstrong, L., Walter, T., Stojkovic, P., Przyborski, S., Herbert, M., Murdoch, A., Strachan, T. and Lako, M. (2005). Downregulation of NANOG induces differentiation of human embryonic stem cells to extraembryonic lineages. *Stem Cells* **23**, 1035-43.

Ivanova, N., Dobrin, R., Lu, R., Kotenko, I., Levorse, J., DeCoste, C., Schafer, X., Lun, Y. and Lemischka, I. R. (2006). Dissecting self-renewal in stem cells with RNA interference. *Nature* **442**, 533-8.

Lee, J., Go, Y., Kang, I., Han, Y. M. and Kim, J. (2010). Oct-4 controls cell-cycle progression of embryonic stem cells. *Biochem. J.* **426**, 171-81.

Loh, Y. H., Wu, Q., Chew, J. L., Vega, V. B., Zhang, W., Chen, X., Bourque, G., George, J., Leong, B., Liu, J. et al. (2006). The Oct4 and Nanog transcription network regulates pluripotency in mouse embryonic stem cells. *Nat. Genet.* **38**, 431-40.

Lowry, W.E. and Quan, W.L. (2010). Roadblocks en route to the clinical application of induced pluripotent stem cells. *J. Cell Sci.* **123**, 643-51

Marson, A., Levine, S. S., Cole, M. F., Frampton, G. M., Brambrink, T., Johnstone, S., Guenther, M. G., Johnston, W. K., Wernig, M., Newman, J. et al. (2008). Connecting microRNA genes to the core transcriptional regulatory circuitry of embryonic stem cells. *Cell* **134**, 521-33.

Mitsui, K., Tokuzawa, Y., Itoh, H., Segawa, K., Murakami, M., Takahashi, K., Maruyama, M., Maeda, M. and Yamanaka, S. (2003). The homeoprotein Nanog is required for maintenance of pluripotency in mouse epiblast and ES cells. *Cell* **113**, 631-42.

Pan, G. and Thomson, J. A. (2007). Nanog and transcriptional networks in embryonic stem cell pluripotency. *Cell Res.* **17**, 42-9.

Pauklin, S., Pederson, R.A. and Vallier, L. (2011). Mouse pluripotent stem cells at a glance. *J. Cell Sci.* **124**, 3727-32.

Peitz, M., Munst, B., Thummer, R. P., Helfen, M. and Edenhofer, F. (2014). Cell-permeant recombinant Nanog protein promotes pluripotency by inhibiting endodermal specification. *Stem Cell Res.* **12**, 680-9.

Piestun, D., Kochupurakkal, B. S., Jacob-Hirsch, J., Zeligson, S., Koudritsky, M., Domany, E., Amariglio, N., Rechavi, G. and Givol, D. (2006). Nanog transforms NIH3T3 cells and targets cell-type restricted genes. *Biochem. Biophys. Res. Commun.* **343**, 279-85.

Rodriguez-Viciana, P., Warne, P. H., Khwaja, A., Marte, B. M., Pappin, D., Das, P., Waterfield, M. D., Ridley, A. and Downward, J. (1997). Role of phosphoinositide 3-OH kinase in cell transformation and control of the actin cytoskeleton by Ras. *Cell* **89**, 457-67.

Sato, T., Okumura, F., Ariga, T. and Hatakeyama, S. (2012). TRIM6 interacts with Myc and maintains the pluripotency of mouse embryonic stem cells. *J. Cell Sci.* **125**, 1544-55.

Saunders, A., Faiola, F. and Wang, J. (2013). Concise review: pursuing self-renewal and pluripotency with the stem cell factor Nanog. *Stem Cells* **31**, 1227-36.

Shan, J., Shen, J., Liu, L., Xia, F., Xu, C., Duan, G., Xu, Y., Ma, Q., Yang, Z., Zhang, Q. et al. (2012). Nanog regulates self-renewal of cancer stem cells through the insulin-like growth factor pathway in human hepatocellular carcinoma. *Hepatology* **56**, 1004-14.

Silva, J., Chambers, I., Pollard, S. and Smith, A. (2006). Nanog promotes transfer of pluripotency after cell fusion. *Nature* **441**, 997-1001.

Silva, J., Nichols, J., Theunissen, T. W., Guo, G., van Oosten, A. L., Barrandon, O., Wray, J., Yamanaka, S., Chambers, I. and Smith, A. (2009). Nanog is the gateway to the pluripotent ground state. *Cell* **138**, 722-37.

Singh, A. M., Hamazaki, T., Hankowski, K. E. and Terada, N. (2007). A heterogeneous expression pattern for Nanog in embryonic stem cells. *Stem Cells* **25**, 2534-42.

Sun, H., Lesche, R., Li, D. M., Liliental, J., Zhang, H., Gao, J., Gavrilova, N., Mueller, B., Liu, X. and Wu, H. (1999). PTEN modulates cell cycle progression and cell survival by regulating phosphatidylinositol 3,4,5,-trisphosphate and Akt/protein kinase B signaling pathway. *Proc. Natl. Acad. Sci. USA* **96**, 6199-204.

Takahashi, K., Mitsui, K. and Yamanaka, S. (2003). Role of ERas in promoting tumour-like properties in mouse embryonic stem cells. *Nature* **423**, 541-5.

Tanaka, Y., Era, T., Nishikawa, S. and Kawamata, S. (2007). Forced expression of Nanog in hematopoietic stem cells results in a gammadeltaT-cell disorder. *Blood* **110**, 107-15.

Thier, M., Munst, B. and Edenhofer, F. (2010). Exploring refined conditions for reprogramming cells by recombinant Oct4 protein. *Int. J. Dev. Biol.* **54**, 1713-21.

Thier, M., Munst, B., Mielke, S. and Edenhofer, F. (2012a). Cellular reprogramming employing recombinant sox2 protein. *Stem Cells Int.* **2012**, 549846.

Thier, M., Worsdorfer, P., Lakes, Y. B., Gorris, R., Herms, S., Opitz, T., Seiferling, D., Quandel, T., Hoffmann, P., Nothen, M. M. et al. (2012b). Direct conversion of fibroblasts into stably expandable neural stem cells. *Cell Stem Cell* **10**, 473-9.

Ying, Q. L., Nichols, J., Evans, E. P. and Smith, A. G. (2002). Changing potency by spontaneous fusion. *Nature* **416**, 545-8.

Zaehres, H., Lensch, M. W., Daheron, L., Stewart, S. A., Itskovitz-Eldor, J. and Daley, G. Q. (2005). High-efficiency RNA interference in human embryonic stem cells. *Stem Cells* **23**, 299-305.

Zhang, J., Wang, X., Chen, B., Suo, G., Zhao, Y., Duan, Z. and Dai, J. (2005). Expression of Nanog gene promotes NIH3T3 cell proliferation. *Biochem. Biophys. Res. Commun.* **338**, 1098-102.

Figures

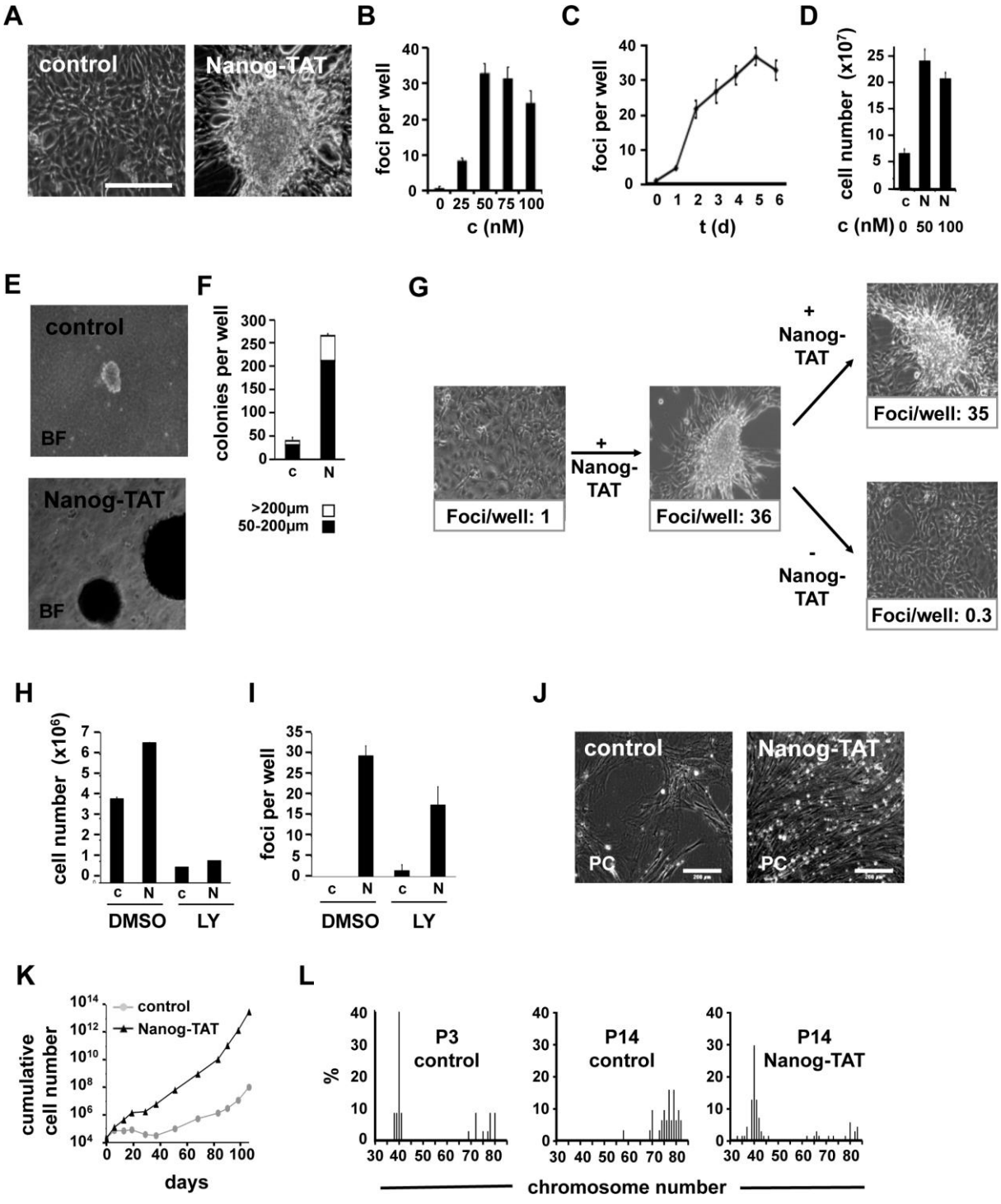

Fig. 1. Nanog-TAT induces anchorage-independent growth of NIH 3T3 cells and enhanced proliferation of mouse fibroblast cells.

(A) NIH 3T3 cells form foci in the presence of cell-permeant Nanog-TAT. NIH 3T3 cells were cultured with 100 nM Nanog-TAT (Peitz et al., 2014) for 8 days; normal

medium served as control. (B) Foci formation is Nanog-TAT concentration dependent. NIH 3T3 cells were cultured with different concentrations of Nanog-TAT and numbers of foci per well were determined after 8 days. Data are means +/- s.e.m. n = 3. (C) Time dependency of Nanog-TAT induced foci formation. NIH 3T3 cells were treated with 50 nM Nanog-TAT for 1–6 days as indicated and in the following Nanog-TAT was withdrawn. Foci formation was quantified after a total culture time of 6 days. Data are means +/- s.e.m. n = 3. (D) Effect of Nanog-TAT on the proliferation of NIH 3T3 cells. To investigate the effects of Nanog-TAT on the proliferation of NIH 3T3 cells, $7.5x10^4$ NIH3T3 cells were plated in 3.5 cm^2 cell culture dishes and cultured with Nanog-TAT for 10 days; normal medium served as control. Equal cell numbers were replated on day 3 and 7. Cumulative cell numbers are shown. Data are means +/- s.e.m., n = 3. c: control; N: Nanog-TAT. (E,F) Nanog-TAT induces anchorage-independent growth in soft agar. NIH 3T3 cells grown for 6 days with 100 nM Nanog-TAT or control media were cultured in soft agar. After 19 days colonies with a diameter >50 µm and >200 µm were counted. Data are means +/- s.e.m. n = 3. (G) Nanog-TAT induced foci formation is reversible. NIH 3T3 cells growing as a monolayer in control media were suspended to a single cell suspension and replated in the presence of Nanog-TAT. The resulting NIH 3T3 foci culture was again replated as a single cell suspension and cultured in the presence or absence of Nanog-TAT. Data of counted foci are means, n = 3. (H) Inhibition of growth promoting effect of Nanog-TAT by PI3K inhibitor LY294002. NIH 3T3 cells were cultured in media with or without 50 nM Nanog-TAT containing DMSO or 10 µM LY294002 for 6 days. Equal cell numbers were replated on day 3. Cumulative cell numbers are shown. Data are means +/- s.e.m., n = 3. (I) Foci formation of Nanog-TAT treated NIH 3T3 cells in the presence and absence of LY294002. Foci were counted after 6 days (mock) and after 9 days (LY294002). Data are means +/- s.e.m., n = 3. c: control; N: Nanog-TAT; LY: PI(3)K-inhibitor LY294002; DMSO: di-methylsulfoxide. (J,K) Primary Oct4-GiP MEF cells show enhanced proliferation in the presence of Nanog-TAT. Oct4-GiP MEFs were cultured either in medium containing Nanog-TAT (50–100 nM) or control medium for 106 days. Equal cell numbers were replated after each passage and cumulative cell numbers were determined. (J) 50 days old fibroblasts are shown in the phase contrast (scale bar 200 µm). A representative proliferation analysis via growth curve is depicted in (K). (L) Nanog-TAT-induced bypass of cellular senescence is associated with

chromosomal stability in Oct4-GiP MEF cells. Metaphases of high passages (P14) of Nanog-TAT treated (*right*) and untreated cells (*middle*) were prepared and chromosomes counted. A low passage (P3) of untreated cells (*left*) served as a control. Percentages of chromosome numbers per nuclei are given. Quantitative evaluation of the counted metaphases (P3: n = 37; control P14: n = 32; Nanog-TAT P14: n = 71).

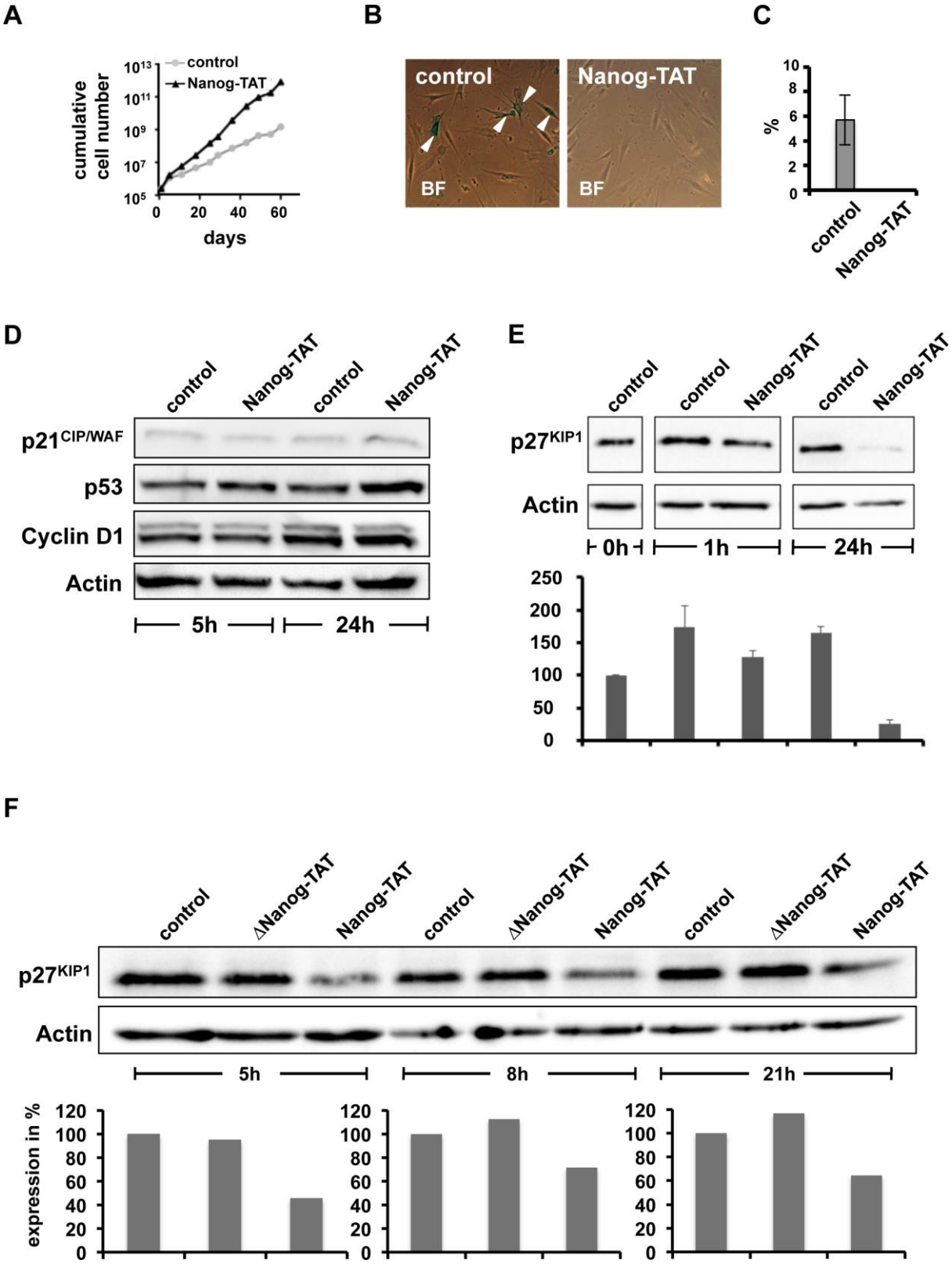

Fig. 2. Nanog suppresses senescence in primary fibroblasts coinciding with low levels of cell cycle kinase inhibitor $p27^{KIP1}$.

(A) Human primary fibroblast cells (MP-hADF) show enhanced proliferation in the presence of Nanog-TAT. Human fibroblasts were cultured in the medium containing 100 nM Nanog-TAT or in control MEF medium. Equal cell numbers were replated after each passage and cumulative cell numbers were determined. A representative proliferation analysis via growth curve is depicted. Cumulative cell numbers are shown. (B) A significant portion of primary human dermal fibroblasts cultured with control medium exhibit senescence-associated SA-β-gal activity whereas cells cultured with 100 nM Nanog-TAT do not stain for SA-β-gal. Magnification for F: 20x; BF: bright field. (C) The quantification of SA-β-gal positive cells in the absence or presence of Nanog-TAT is depicted. 5.7% of cells cultivated with control medium are positive for SA-β-gal, whereas no SA-β-gal positive cells could be observed in the presence Nanog-TAT. (D,E) The expression levels of different key molecules involved in the cell cycle control were assessed in response to Nanog protein transduction. Oct4-GiP MEFs were synchronized and treated with Nanog-TAT-supplemented medium (100 nM). After 5h and 24h, respectively, fibroblasts were harvested and subjected to immunoblot analysis employing antibodies as depicted. Fibroblasts treated with Nanog-TAT show no striking differences in expression of $p21^{CIP/WAF}$, p53, or Cyclin D1 compared to Oct4-GiP MEFs treated with control medium. Actin served as a loading control. (E) Oct4-GiP MEFs were synchronized and incubated with control medium or 100 nM Nanog-TAT. After distinct time points, Oct4-GiP MEFs were harvested and subjected to immunoblot analysis with $p27^{KIP1}$ antibody. A representative immunoblot is shown (top panel) showing that $p27^{KIP1}$ is consistently down-regulated upon Nanog-TAT treatment. Actin served as a loading control. Densitometric analysis of $p27^{KIP1}$ expression levels is presented (bottom panel). n = 3. (F) Oct4-GiP MEFs were synchronized and incubated with medium only (control), medium containing 50 nM control protein ΔNanog-TAT as well as Nanog-TAT for indicated periods of time. Upon culture of Oct4-GiP MEFs with Nanog-TAT, $p27^{KIP1}$ expression is down-regulated after 5h, 8h and 21h. Culture of Oct4-GiP MEFs with ΔNanog-TAT does not change protein expression levels of $p27^{KIP1}$ compared to cells treated with control medium (top). The immunoblot was quantified densitometrically and quantification of $p27^{KIP1}$expression is depicted

(bottom). After 5h of Nanog-TAT treatment the expression of $p27^{KIP1}$ is decreased to around 45%, after 8h $p27^{KIP1}$ expression is reduced to approximately 70% and after 21h of Nanog-TAT culture $p27^{KIP1}$ expression is diminished to around 65%.

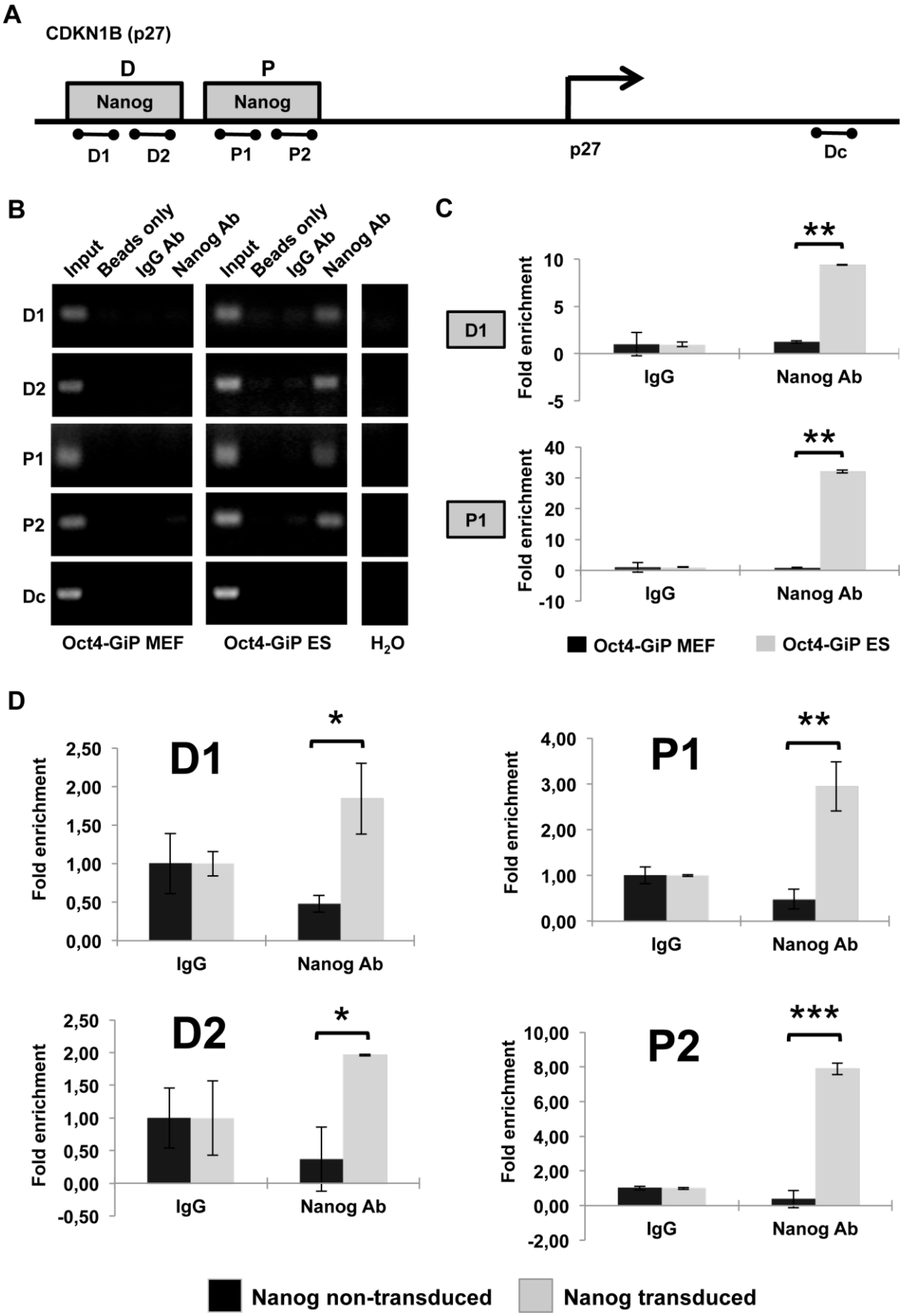

Fig. 3. ChIP analysis reveals Nanog binding sites regulating p27^{KIP1} expression. (A) Schematic representation (not drawn to scale) of the p27 genomic locus (RefSeq: NM_009875) highlighting the location of putative Nanog binding sites designated 'D (primer pairs designated as D1 and D2)' and 'P (primer pairs designated as P1 and P2)' in the upstream region of the p27 gene (Chen et al., 2008; Marson *et al.,* 2008). PCR primer pairs were designed for these sites for ChIP analyses (dumbbell shaped; Table S2). (B) ChIP analysis reveals that Nanog protein in ES cells binds within the upstream region of the p27 gene. Oct4-GiP MEF and Oct4-GiP ES cells were cultured, harvested and processed for ChIP analysis with beads only, IgG and Nanog antibody. Oct4-GiP MEF cell line was used as a negative control. Input DNA (10%) was used as a control for ChIP. Beads only and IgG served as negative controls. Putative Nanog binding regions were amplified by designed primer pairs (D1, D2, P1 and P2). Primer pairs were also designed randomly in the 3´UTR region of the p27 gene to serve as a negative (desert) control (Dc). (C) Quantitative PCR (q-PCR) analysis on the ChIP samples explained in (B) using primers pairs of P1 and D1 to amplify the Nanog binding p27^{KIP1} sites. q-PCR was also performed on the Dc primer set but no amplification was observed other than the input samples (data not shown). 2 independent biological replicates were performed for ChIP analysis. Statistical analysis to calculate p-value was carried out using a two-tailed test; p-value: ** $p < 0.01$. (D) Quantitative PCR (q-PCR) analysis on the ChIP samples explained in (B) derived from MEF cells transduced with 100 nM Nanog-TAT. Non-transduced fibroblasts kept in standard media served as controls. Oct4-GiP MEF (passage 3) were treated with dialysis buffer only and with 100 nM Nanog-TAT for 10h, harvested and processed for ChIP analysis with IgG and Nanog antibody. Cells were washed with heparin to remove extracellularly bound Nanog-TAT protein before harvesting fibroblasts. Input DNA (10%) was used as a control for the ChIP. IgG served as negative control. Putative Nanog binding regions upstream to p27 transcriptional start site were amplified by primer pairs (designated as D1, D2, P1 and P2; Table S2). Primer pairs were also designed randomly in the 3´UTR region of the p27 gene to serve as a negative (desert) control (Dc) but no amplification was observed other than the input samples (data not shown). 2 independent biological replicates were performed for ChIP analysis. Statistical analysis to calculate p-value was carried out using a two-tailed test; p-value: * $p < 0.05$; ** $p < 0.01$; *** $p < 0.001$.

SUPPLEMENTARY TABLES:

Table S1: Primers used for RT-PCR (this table is related to Figure S2).

Genes	Primer sequence (5´-3´)
$p27^{KIP1}$	**F:** TCTCTTCGGCCCGGTCAAT **R:** GGGGCTTATGATTCTGAAAGTCG
p53	**F:** TGAAACGCCGACCTATCCTTA **R:** GGCACAAACACGAACCTCAAA
$p21^{CIP/WAF}$	**F:** CTGAGGATGAACAGTAACAACCG **R:** CTGGGAAGATAGAGCGAAGCC
$p16^{INK4a}$	**F:** GCTGCAGACAGACTGGCCA **R:** GTCCTCGCAGTTCGAATCTG
FGF receptor 1 (FGF-R1)	**F:** GGTGCTTCATCTACGGAATGTC **R:** TGATGGGAGAGTCCGATAGAGT
GAPDH	**F:** ACGACCCCTTCATTGACCTCAACT **R:** ATATTTCTCGTGGTTCACACCCAT

Table S2: Primer pairs used for ChIP analysis (this table is related to Figure 3).

Primers	Primer Sequence (5´-3´)
D1	**F:** CTTCTCATCCCAAGTCCACA **R:** AGACTACCTGGGTAGGTAATTTGG
D2	**F:** GGCTGGAGTCATCAGAAAGC **R:** GGCCATAAGACAAAGGAGGA
P1	**F:** TGAAGAGATTGGGGGTATGG **R:** AGCCCCAACTGTGTCTGAAG
P2	**F:** CAGTTGGGGCTCATAATTGC **R:** AGAACACCTGCGTGGAAGAT
Dc	**F:** AGACACTGAAAATTATACTAA **R:** GTAACAATAATTGGCATCTTT

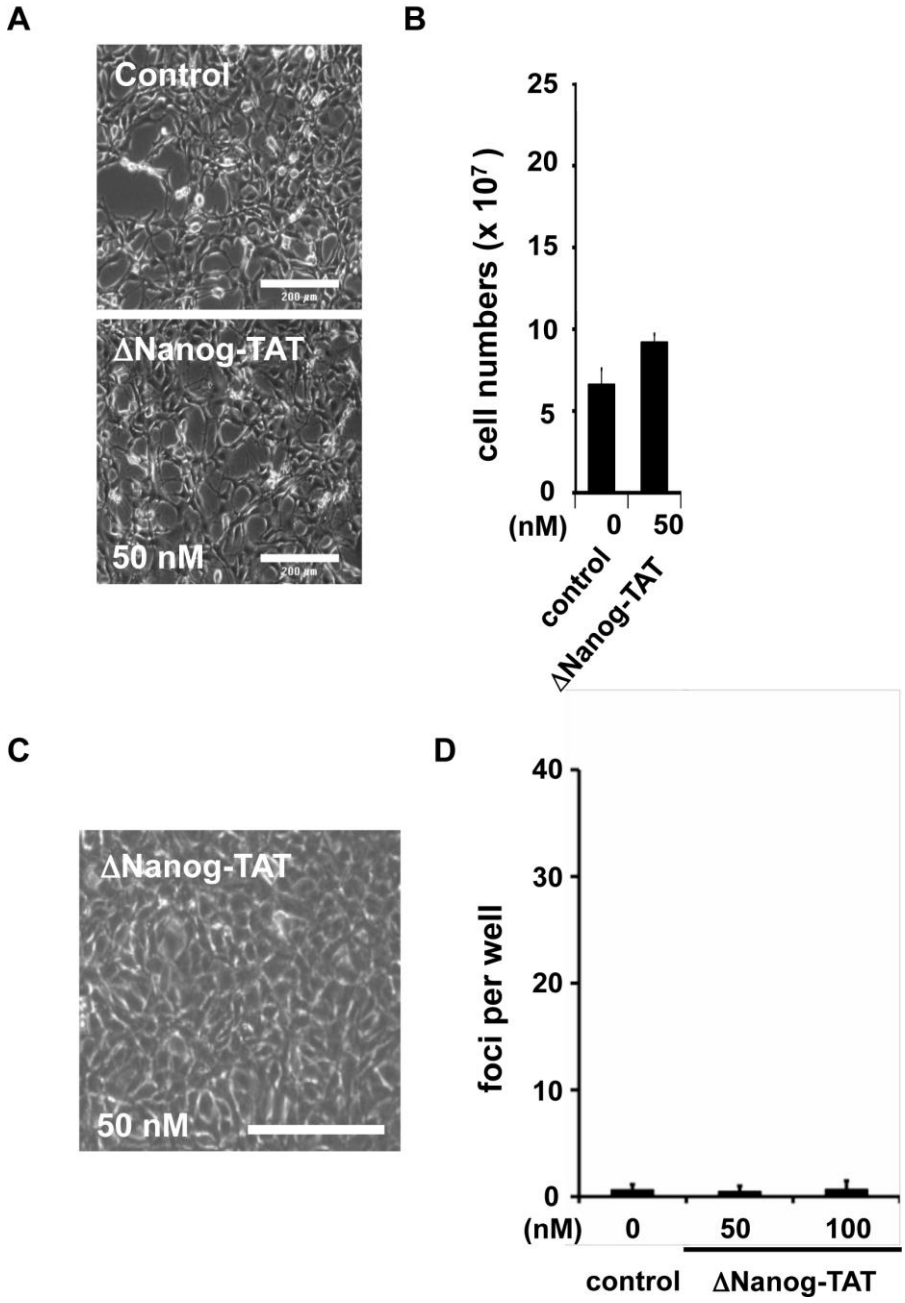

Figure S1: ΔNanog-TAT fails to enhance proliferation or generate cell-foci in NIH3T3 cells.

The deletion of the 65 aa long homeobox domain should attenuate binding of the deletion mutant to the DNA, i.e. ΔNanog-TAT should not exhibit functionality when compared to Nanog-TAT. (A,B) Effect of ΔNanog-TAT on the proliferation of NIH 3T3 cells. To investigate the effects of ΔNanog-TAT on the proliferation of NIH 3T3 cells, $7.5x10^4$ cells were plated in 3.5 cm^2 cell culture dishes with both control medium and 50 nM of ΔNanog-TAT recombinant protein for 10 days and were replated on day 3 and 7. Normal medium served as control. After 10 days, phase contrast images (A) were taken and and the cumulative cell number was determined and shown in (B). Data are means +/- s.e.m. n = 3. Scale: 200 µm. (C,D) NIH 3T3 cells could not form foci in the presence of ΔNanog-TAT. (C) Phase contrast images of NIH 3T3 cells cultivated with 50 nM ΔNanog-TAT for 10 days. (D) NIH 3T3 cells were cultivated with 50 and 100 nM concentrations of ΔNanog-TAT and numbers of foci per well were determined after 8 days; normal medium served as control. Data are means +/- s.e.m. n = 3.

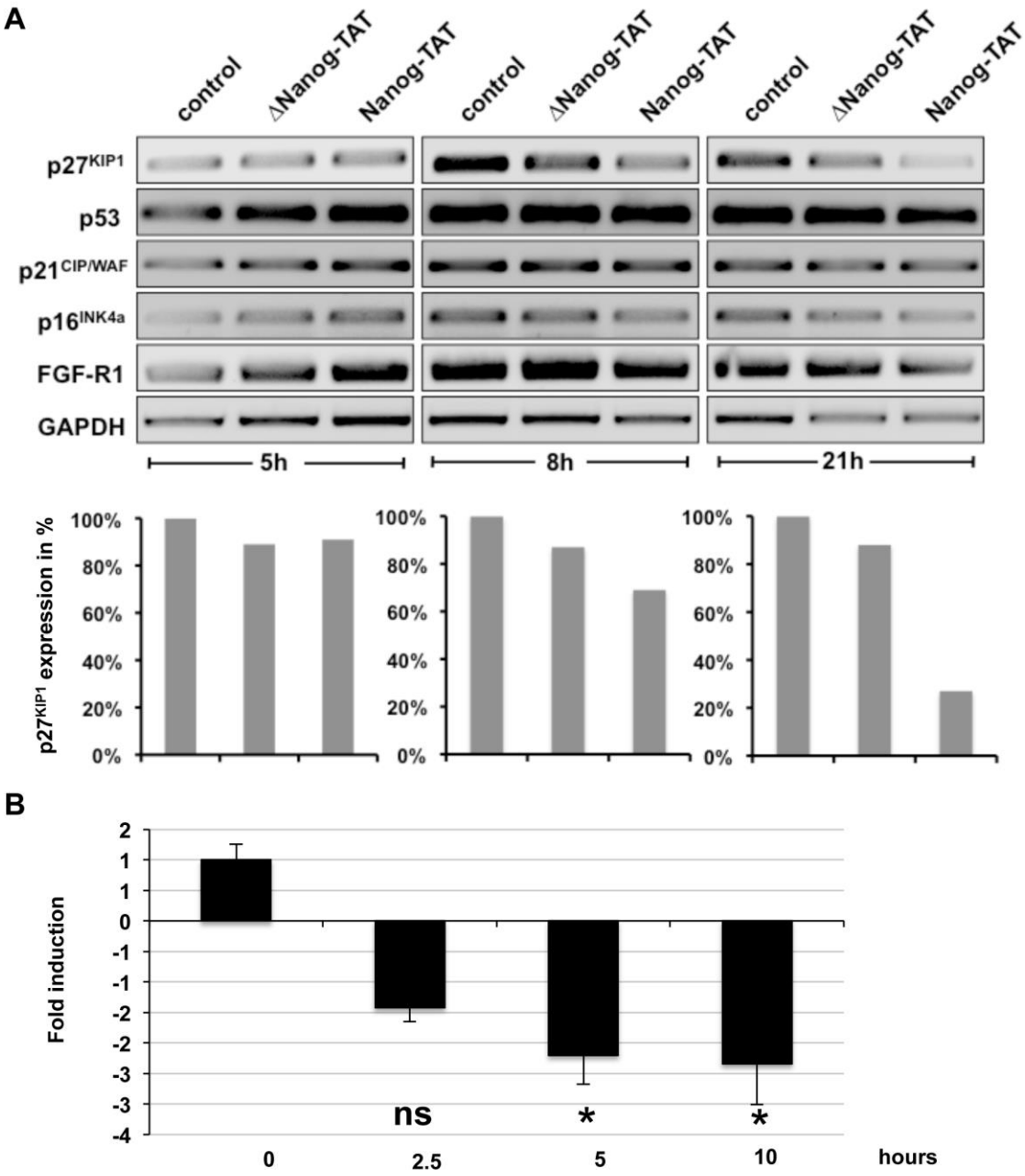

Figure S2: Nanog-TAT delivery results in decreased expression levels of $p27^{KIP1}$.

(A) MEFs were synchronized and cultivated with control medium, ΔNanog-TAT and Nanog-TAT, respectively. After 5, 8 and 21h the fibroblasts were harvested and the expression levels of different key molecules involved in proliferation as well as cell cycle regulation were assessed via RT-PCR. No change in transcription levels is apparent for p53, $p21^{CIP/WAF}$, $p16^{INK4a}$ and FGF-receptor 1. Modulation of $p27^{KIP1}$ mRNA expression is apparent in Oct4-GiP MEFs upon cultivation with Nanog-TAT (top). The transcriptional expression level of $p27^{KIP1}$ was quantified densitometrically (bottom). Results are normalized to GAPDH. FGF-R1: FGF receptor 1; GAPDH: Glyceraldehyde 3-phosphate dehydrogenase. (B) Fold change expression levels of $p27^{KIP1}$ transcripts by qPCR. Oct4-GiP MEFs were synchronized and subsequently cultivated with control medium or 100 nM Nanog-TAT. After 0, 2.5, 5 and 10h, fibroblasts were harvested and the expression levels of $p27^{KIP1}$ were assessed via qPCR. Before harvesting fibroblasts, cells were washed with heparin to remove extracellularly bound Nanog-TAT protein. Expression levels of $p27^{KIP1}$ were down-regulated after Nanog-TAT treatment compared to untreated fibroblasts. $p27^{KIP1}$ gene expression levels are expressed as Log2 fold changes based on Ct calculation using GAPDH as a house-keeping gene and non-transduced fibroblasts (0 hours) as a negative control. n = 2. Statistical analysis to calculate p-value was carried out using a two-tailed test; p-value: ns - not significant; * $p < 0.05$.